

# Single-Mechanism Rate Theory for Dynamic Strain Aging in fcc Metals

M. A. Soare and W. A. Curtin<sup>1</sup>

Division of Engineering, Brown University, Providence RI 02912

## Abstract

A full thermal-activation rate theory for dynamic strain aging is developed for the case where a single rate-dependent strengthening mechanism controls dislocation motion in a material and where that mechanism is modified by additional time-dependent strengthening by, e.g., solute diffusion. The analysis shows that negative strain rate sensitivity cannot be obtained within such a framework, a conclusion previously reached by Hähner [1]. However, the strain rate sensitivity can be greatly reduced over a range of strain rates, making negative strain rate sensitivity more accessible by other mechanisms. In addition, the aging mechanism naturally gives rise to an instantaneous positive strain rate sensitivity and stress relaxation behavior under strain-rate jump conditions, putting the concepts advanced by McCormick [2, 3] on a quantitative footing. Finally, the model shows that non-steady state strain histories can also give rise to apparent material softening. The results here set the stage for subsequent work wherein consideration of multiple strengthening mechanisms (solute and forest hardening) operating together and with the same underlying aging mechanism can predict negative strain rate sensitivity, and its strain-rate, strain, temperature, and concentration-dependence, in quantitative agreement with data in Al-Mg solid solution alloys.

**Keywords:** Thermally activated processes, Dislocations, Constitutive Equations, Solute strengthening.

---

<sup>1</sup> Corresponding author. Tel: +401 863 1418; fax:+1 401 863 9025

## 1. Introduction

In fcc metals, plastic flow is governed by the motion of dislocations and the strain rate dependence is envisioned to be governed by the thermally-activated release of dislocations from local pinning points. These pinning points could be other dislocations forming a forest, precipitate particles, solute atoms, or other microstructural defects in the material. Standard analyses study a single typical dislocation and the energy landscape it encounters during motion [1, 2, 4-6] and are aimed at steady-state deformation. Mobile dislocations are envisioned to be pinned for an average waiting time  $\bar{t}_w$  after which they move rapidly through the material to the next pinning configuration. Under steady-state conditions (constant strain rate), the Orowan equation  $\dot{\epsilon} = \rho_m b \bar{v}$  relating strain rate to average dislocation velocity  $\bar{v}$  becomes  $\dot{\epsilon} = \rho_m b \bar{d} / \bar{t}_w = \Omega / \bar{t}_w$  where  $\bar{d}$  is the average flight distance between pinning points [7, 8]. For pinning by forest dislocations,  $\bar{d} \sim \rho_f^{-1/2}$  so that  $\Omega = \rho_m b \rho_f^{-1/2}$  is a function of the mobile and forest dislocation densities that evolve with plastic strain. The average waiting time  $\bar{t}_w$  is considered to be the inverse of the average rate of escape over the energy barrier presented by the pinning obstacles. Specifically,  $\bar{t}_w = \nu_0^{-1} e^{\Delta E / kT}$  where  $\Delta E$  is the energy barrier and  $\nu_0$  a fundamental attempt frequency. The energy barrier is determined by the resisting force versus dislocation position imposed by the obstacle and the local stress  $\tau$  acting on the dislocation, i.e.  $\Delta E = \Delta E(\tau)$ . Various energy barrier models have been described by Friedel [9], Kocks and collaborators [4], Estrin and McCormick [3], Springer et al. [6], and are associated with various types of obstacles. The resulting strain rate versus stress is then of the general form

$$\dot{\epsilon} = \dot{\epsilon}_0 \exp(-\Delta E(\tau) / kT). \quad (1a)$$

A recent monograph [10] examines the success of these models for solute strengthening against experiments in a variety of metal alloys. Another notable success is the rate dependence of forest hardening as revealed by Cottrell and Stokes [11].

The strain-rate sensitivity (SRS), defined here as the dimensionless parameter  $m = d(\ln \tau) / d(\ln \dot{\epsilon})$ , and the activation volume, defined as  $V_{act} = -d(\Delta E) / d\tau = kT / (m\tau)$ , provide insight into the mechanisms determining the energy barrier  $\Delta E$ . For instance, recent work in nanoscale twinning of Cu [12] has shown that dislocation reactions at the twin boundary have an activation volume comparable to that derived experimentally. Other recent work on nanocrystalline materials [13] has also used the activation volume to deduce mechanisms. Thus, the thermally-activated release of individual dislocations as the rate controlling process is well-established in many systems.

When time-dependent aging occurs in a material, the rate dependence of strengthening is usually treated in a more-approximate manner. In particular, in alloys showing dynamic strain aging attributed to solute diffusion toward dislocations during the waiting time  $\bar{t}_w$ , the starting point for most models is the assumption of a strain-rate law

$$\dot{\epsilon} = \dot{\epsilon}_0 \exp(-\Delta E(\tau, C) / kT) \quad (1b)$$

where the activation energy is related to an internal variable  $C$  accounting for the aging behavior.  $C$  is commonly related to the time-dependent solute concentration accumulated around a dislocation during an aging time  $t_a$  as

$$C(t_a) = C_m \left[ 1 - \exp(-(C_0 / C_m)(t_a / t_d)^n) \right] \quad (2)$$

where  $t_a$  is the typical dislocation aging time,  $t_d$  is a characteristic solute diffusion time in the presence of the dislocation,  $C_0$  is the alloy solute composition,  $C_m$  is the saturation value of the solute concentration at the dislocation core, and  $n$  is a parameter usually taken to be 2/3 or 1/3 [7, 8, 11, 14-16]. To eliminate the explicit time dependence in Eq. 2, under steady-state conditions the aging time is set equal to the average waiting time,  $t_a = \bar{t}_w = \Omega / \dot{\epsilon}$ , which when substituted into Eq. 1b gives a closed equation. To obtain a specific and usable form in the absence of a direct knowledge of the concentration dependence of the energy barrier  $\Delta E(\tau, C)$ , the activation enthalpy is often further linearized around some unspecified reference stress  $\tau_r$  [3, 17, 18] and around zero solute concentration as

$$\frac{\Delta E(\tau, C)}{kT} = \left. \frac{\partial(\Delta E / kT)}{\partial \tau} \right|_{\tau_r, 0} (\tau - \tau_r) + \left. \frac{\partial(\Delta E / kT)}{\partial C} \right|_{\tau_r, 0} C(t_a = \Omega / \dot{\epsilon}) \quad (3)$$

The coefficient of the first term on the right hand side of Eq. 3 is then identified as  $m_p / \tau_r$  and is related to the normal positive strain rate sensitivity. The coefficient of the second term on the right hand side of Eq. 3 is denoted as  $H$  and is related to the dynamic strain aging. Inserting Eq. 3 into Eq. 1b and re-arranging then leads to the relation between strain rate and stress usually postulated in the literature,

$$\tau = \tau_r (1 + m_p \ln(\dot{\epsilon} / \dot{\epsilon}_0) + m_p H C(\dot{\epsilon})). \quad (4)$$

Since  $C(\dot{\epsilon}) = C_m \left[ 1 - \exp(-(C_0 / C_m)(\Omega / \dot{\epsilon} t_d)^{2/3}) \right]$  shows negative strain rate sensitivity (nSRS) *by construction*, the overall material response can show nSRS if the combination  $HC$  is large enough to overcome the positive strain rate sensitivity  $m_p$ .

At the macroscopic scale the dynamic strain aging mechanisms (DSA) can lead to undesirable inhomogeneous flow and plastic instabilities. Localization bands may appear in the material, each of these bands leading to a serration in the stress-strain curve (this process is well known as the Portevin-Le Châtelier effect) [1, 7, 17-20]. For this reason, a model that can incorporate the aging mechanisms taking place at small-scale level and that is able to predict the non-steady state behavior of these materials is essential. A correct description of the non-steady-state behavior, associated with strain jumps and PLC effects in the real material, is required for any numerical model to be well-posed and not be controlled by mesh refinements or time increments used in the numerics.

To handle non-steady-state conditions, the aging time  $t_a$  has usually been assumed to evolve with the strain rate via an ad-hoc first order kinetic model given by [2, 3, 21-23]:

$$\frac{dt_a}{dt} = - \left( \frac{t_a(t) - t_w(t)}{t_w(t)} \right) \quad (5)$$

where  $t_w(t) = \frac{\Omega}{\dot{\epsilon}(t)}$  is the steady-state waiting time that would exist for a constant strain rate having the value  $\dot{\epsilon}(t)$ . Eq. 5 is argued to be due to the relaxation of the solute diffusion to the new imposed strain rate, although there is no direct connection to any microscopic mechanism.

The manifestations of Eqs. 1-5 at the macroscopic scale are generally consistent with experimental observations. However, this agreement is obtained largely by construction. Moreover, few of the assumptions are grounded in the underlying physics of the dislocation motion and solute diffusion. First, there is a very weak physical basis for making the direct association between the solute concentration and proportional changes in the dislocation activation enthalpy. Second, there is only a qualitative basis for using the average waiting time as the aging time. Third, the linearization is purely for mathematical convenience. Fourth, the postulated non-steady-state relaxation behavior cannot be motivated by considerations of solute diffusion since the solutes are not cognizant of the macroscopic applied strain rate; any single dislocation is accumulating solutes by diffusion in a manner that is independent of the overall strain rate. The strain-rate dependence should arise from the interplay of the rate of escape of a dislocation from its local energy well, as driven by the applied stress, and the rate of increase in the energy barrier as solute diffusion proceeds.

While phenomenologically attractive, the limitations of the above models motivate us to proceed more precisely with a rate theory that does not start from Eq. 1b and does not need to invoke additional assumptions such as Eq. 5 for non-steady-state behavior. Our model is developed within exactly the same framework as the prior models by assuming that the overall plastic strain rate follows the Orowan relationship and that each mobile dislocation can be treated as an independent entity. Using a proper rate theory, we find quite generally that negative strain rate sensitivity cannot be obtained when there is a single rate-dependent strengthening mechanism operating in the material. This conclusion was also reached by Hähner [1] in an analysis similar to the present one. However, we are able to numerically solve the resulting integral equations and make further quantitative assessments of the rate model and to show several new features, as follows. First, the rate dependence can be decreased significantly when aging mechanisms operate even though  $m > 0$  holds at all times. Second, the model predicts a transient stress relaxation history under strain-rate-jump tests, with transient times that differ from the assumption of Eq. 5 and other estimates. Third, under non-steady-state strain history, the material response can be complex due to the competition between the strain-rate variations and the fundamental material aging rate. Although negative SRS is not obtained, these results provide an important basis for our subsequent development of new physically-based models that can quantitatively account for the SRS, both positive and negative, as a function of

temperature, strain rate, strain, and solute concentration in solid-solution-strengthened alloys. This important new model is described in a companion paper.

## 2. Kinetic Model for the Strain Rate Dependence of Plastic Flow with Aging

We envision a single mechanism pinning the dislocation. Whether that mechanism is solute strengthening, forest hardening, or some other mechanism is not important for the discussion. This mechanism is then augmented by an aging phenomenon that acts directly in concert with the underlying strengthening mechanism. For instance, if the strengthening is by static solutes pinning the mobile dislocations, then the aging is by diffusion of solutes to those pinning regions, influencing the solute-induced energy barrier. If the strengthening is by forest pinning, then the aging is by diffusion of solutes to the junctions, influencing the junction energy barrier. An important aspect of the analysis is that the aging starts when the dislocation is first pinned at the obstacle.

Proceeding with the analysis, at stresses below the zero temperature flow stress, a dislocation is assumed to move only by thermal activation across an energy barrier. The energy barrier  $\Delta E$  is a function of the current applied stress, which depends on the current time  $t$ , and the elapsed time  $t - t_p$  during which the dislocation has been pinned in the energy well of the strengthening mechanism. Within transition rate theory, the instantaneous rate of escape of an individual dislocation over the energy barrier at time  $t$  and stress  $\tau(t)$  is given by

$$\nu(\tau(t), t - t_p) = \nu_0 \exp\left(-\frac{\Delta E(\tau(t), t - t_p)}{kT}\right) \quad (6)$$

where  $\nu_0$  is the attempt frequency and  $t_p$  is the time at which the dislocation becomes pinned at the obstacle. We now calculate the probability per unit time  $p(\tau(t), t - t_p)$  that the dislocation actually escapes at stress  $\tau$  and time  $t$ . First, the probability of *not* escaping in an infinitesimal increment  $dt'$  at time  $t'$  is  $1 - \nu(\tau(t'), t' - t_p)dt'$ . The probability  $p_s$  that the dislocation has not escaped (i.e. survived at the present pinning site) during the interval  $[t_p, t]$  is then the product of all such incremental probabilities over the interval, which in the limit of  $dt \rightarrow 0$ , can be written as

$$p_s(\tau(t), t - t_p) = \exp\left(-\int_{t_p}^t \nu(\tau(t'), t' - t_p) dt'\right) \quad (7)$$

The probability density per unit time for a dislocation to escape at time  $t$  is then

$$p(\tau(t), t - t_p) = \nu(\tau(t), t - t_p) \exp\left(-\int_{t_p}^t \nu(\tau(t'), t' - t_p) dt'\right) \quad (8)$$

This quantity is a proper probability distribution, being normalized to unity over the interval  $[t_p, \infty)$  for any arbitrary rate of escape. Eq. 8 is well known, for instance, in the

field of electron conduction by multiple trapping in band-gap states in amorphous Si and is generalizable to multiple mechanisms and statistical distributions of trapping [24]. Qualitatively, in the presence of aging at constant stress, the energy barrier increases with time, the escape rate correspondingly decreases with time, and the probability distribution of Eq. 8 is stretched out relative to the non-aging case, becoming smaller at short times where the pre-factor dominates and larger at long times where the integral in the exponential dominates.

To connect the instantaneous rate of escape for a single dislocation to the macroscopic strain rate for both steady-state and non-steady-state conditions, we proceed as follows. Consider a collection of  $N_m$  mobile dislocations  $\{i\}$ , pinned at various obstacles. Denote by  $t_p^i$  the time at which the  $i^{\text{th}}$  dislocation has been pinned. The strain rate at time  $t$  is then the rate of dislocation escape at time  $t$  multiplied by the slip increment  $b\bar{d}$  obtained upon escape and summed over all mobile dislocations in the system,

$$\dot{\epsilon}(t) = b\bar{d} \sum_i \frac{1}{A} p(\tau(t), t - t_p^i) \quad (9)$$

where  $A = N_m / \rho_m$  is the sample area in the plane of the imposed shear deformation. Eq. 9 can be rewritten as

$$\dot{\epsilon}(t) = b\rho_m \bar{d} \sum_i \frac{1}{N_m} p(\tau(t), t - t_p^i) = \Omega \sum_i \frac{1}{N_m} p(\tau(t), t - t_p^i) \quad (10)$$

where  $\Omega = b\rho_m \bar{d}$  is the elementary strain increment produced when all the mobile dislocations accomplish a successful thermally-activated event. The current strain rate thus depends on the prior history of last pinning times and the applied stress history. Considering a distribution in time of such pinning events, with the probability of pinning at time  $t_p$  denoted as  $p_p(t_p)$ , we replace the sum in Eq. 10 by an integral and obtain the strain rate as

$$\dot{\epsilon}(t) = \Omega \int_{-\infty}^t p_p(t_p) p(\tau(t), t - t_p) dt_p \quad (11)$$

The key step now lies in recognizing that the probability of pinning at time  $t_p$  is precisely the rate of release of the dislocation from its prior pinning site at the same time (neglecting the flight time, which is very short). This rate is, in turn, related to the strain rate at that time, so that  $p_p(t_p) = \dot{\epsilon}(t_p) / \Omega$ . Inserting this result into Eq. 11 and using Eq. 8, we obtain the general constitutive equation relating the strain rate to the stress and time history of the energy barriers in the system as

$$\dot{\epsilon}(t) = \int_{-\infty}^t \dot{\epsilon}(t_p) \nu(\tau(t), t - t_p) \exp\left(-\int_{t_p}^t \nu(\tau(t'), t' - t_p) dt'\right) dt_p \quad (12)$$

Eq. 12 is the first main result of this paper.

Before analyzing Eq. 12 in detail, we note that under steady-state conditions, the strain rate cancels out and the resulting equation is an identity. Thus, the steady-state rate cannot be derived directly from Eq. 12 in spite of its generality. We therefore manipulate Eq. 12 to obtain another useful relation between the strain rate, stress, and time. We change variables in Eq. 12 to  $t_a = t - t_p$ ,  $t'' = t' - t_p$ , integrate by parts, and re-arrange the terms to obtain

$$\frac{d}{dt} \left[ \int_0^\infty \dot{\epsilon}(t - t_a) \exp \left( - \int_0^{t_a} \nu(\tau(t'' + t - t_a), t'') dt'' \right) dt_a \right] = 0 \quad (13)$$

which implies that

$$\int_0^\infty \dot{\epsilon}(t - t_a) \exp \left( - \int_0^{t_a} \nu(\tau(t'' + t - t_a), t'') dt'' \right) = Const \quad (14)$$

Under a steady-state strain rate and, thus, constant stress, Eq. 14 shows that

$$Const / \dot{\epsilon} = \int_0^\infty \exp \left( - \int_0^t \nu(\tau, t') dt' \right) dt \quad (15)$$

The right hand side of Eq.15 is, however, exactly the average waiting time  $\bar{t}_w$ , as shown by computing it as the mean of the escape probability,

$$\bar{t}_w = \int_0^\infty t p(\tau, t) dt = \int_0^\infty t \nu(\tau, t) \exp \left( - \int_0^t \nu(\tau, t') dt' \right) dt = \int_0^\infty \exp \left( - \int_0^t \nu(\tau, t') dt' \right) dt \quad (16)$$

We therefore deduce that  $Const = \Omega$ , the elementary strain, and can rewrite Eq. (14) as

$$\Omega = \int_{-\infty}^t \dot{\epsilon}(t_p) \exp \left( - \int_{t_p}^t \nu(\tau(t''), t'' - t_p) dt'' \right) \quad (17)$$

and write the steady-state strain rate in the “usual” form

$$\dot{\epsilon} = \Omega / \bar{t}_w \quad (18)$$

with  $\bar{t}_w$  given by Eq. 16. Eq. 17 is the second main result of this paper.

Eq. 12 or Eq. 17 completely describes the evolution of the strain rate with the applied stress history and any aging that is contained within the time-dependence evolution of the

energy barrier. Eq. 17 is useful for predicting steady-state behavior, as it leads to Eq. 18, while Eq. 12 is useful in dealing with discontinuities in the strain rate. We note clearly that the equivalents of Eqs. 12 and 17 were derived previously by Hähner [1]. Hähner also highlighted the fact that the strain rate sensitivity parameter is positive definite (see below). Thus, our present analysis can be viewed as a different route to the same result, where we have emphasized from the start the specific time dependence of the energy barrier due to aging. In the following sections, we analyze further the behaviors predicted by Eqs. 12 and 17 in the presence of aging effects to elucidate some important features that were not adequately addressed in Hähner’s work and that bear strongly on our subsequent models for negative strain rate sensitivity. We also believe our derivation is useful at this juncture because Hähner’s work was never built upon further. After one companion paper arguing for a “dynamic synchronization” phenomena to obtain negative  $m$ , Hähner and coworkers subsequently devised a completely different model based on a kinetic model for evolution of the energy barrier and have used only that later model in many, if not all, subsequent publications [18, 19, 20, 25].

### 3. Predictions of Strain-Rate Behavior with Aging

#### 3.1 General Features

We now analyze the most important features of the general kinetic model. First, the model should yield the standard rate model for a constant applied stress and in the absence of any aging effects. In this case, the rate  $\nu$  is constant in time and depends only on the stress,  $\nu = \nu(\tau)$ . The inner integrand of Eq.16 is then constant and the integration is trivial, yielding the standard result  $\dot{\epsilon} / \nu(\tau) = \Omega$  which, upon substituting in Eq. 6, yields

$$\dot{\epsilon} = \Omega \nu_0 \exp(-\Delta E(\tau) / kT) \quad (19)$$

which is identical to Eq.1a with  $\dot{\epsilon}_0 = \Omega \nu_0$ . Our model is thus fully consistent with the long-standing kinetic theories of slip in the absence of aging effects.

Second, in the presence of aging, the steady-state strain rate sensitivity can be computed directly from Eqs. 16 and 18, and is always positive. Specifically, the derivative of the strain rate versus the applied stress is

$$\frac{d\dot{\epsilon}}{d\tau} = \frac{d}{d\tau} \left( \frac{\Omega}{\bar{t}_w} \right) = -\frac{\Omega}{\bar{t}_w^2} \int_0^\infty \left( -\int_0^t \frac{d\nu(\tau, t')}{d\tau} dt' \right) \exp \left( -\int_0^t \nu(\tau, t') dt' \right) dt \quad (20)$$

The rate of escape must always be an increasing function of the applied stress, i.e.  $\frac{d\nu(\tau, t')}{d\tau} \geq 0$ . It is not possible to delay dislocation escape over a well-defined barrier by raising the applied stress. An applied stress puts energy into the system and assists in lowering the barrier for motion in the direction of the applied field independent of the form of the energy barrier. All other terms in Eq. 20 are positive and the two negative signs cancel. Therefore, we deduce, on the most general grounds, that

$$\frac{d\dot{\epsilon}}{d\tau} \geq 0 \text{ and } m = \frac{d(\ln(\tau))}{d(\ln(\dot{\epsilon}))} = \frac{\dot{\epsilon}}{\tau} \frac{d(\tau)}{d(\dot{\epsilon})} \geq 0 \quad (21)$$

*i.e. the steady-state the strain rate sensitivity (SRS) parameter  $m$  is always positive, independent of the underlying microscopic details of the time-dependence of the energy barrier.* This conclusion holds when all mobile dislocations are treated equally and independently, which is implicitly assumed in all models to date for the kinetics of slip with or without DSA. We conclude that the steady-state negative SRS is not possible for a collection of non-interacting dislocations within a model that considers the energy barrier to be associated with one single mechanism of pinning. The occurrence of negative SRS must thus rely on a more complex internal dynamics than heretofore has been envisioned. Eq. 21 ( $m > 0$ ) is the third main result of this paper.

In light of Eq. 21 showing  $m > 0$ , the origin of  $m < 0$  in the standard model of Eqs. 1b-3 becomes clear. Eq. 3 is obtained from our result by replacing the aging time variable in the integral in the exponential of Eq. 15 by the *average* waiting time  $\bar{t}_w = \Omega / \dot{\epsilon}$ . However, such a replacement is strictly not valid because it neglects the evolving shape of the escape probability due to aging effects. Thus, a seemingly reasonable assumption completely changes the predicted behavior, yielding a predicted negative SRS that cannot, in reality, be achieved.

### 3.2 Energy Barrier Models

We now apply the model to predict the strain-rate behavior when dislocation aging is controlled by a time-dependent phenomenon that, for specificity, we envision as solute diffusion. To proceed, we require some model for the energy barrier including aging. We start by describing the energy barrier in the absence of aging. We assume the general form proposed by Kocks and collaborators [4] and derivable from a range of models associated with dislocation/obstacle interactions,

$$\Delta E_0(\tau) = \Delta E_0 \left( 1 - \frac{\tau}{\tau_0} \right)^\alpha \quad (22)$$

where  $\Delta E_0$  is the zero stress energy barrier,  $\tau_0$  is the zero temperature strength (*i.e.* the stress at which the barrier becomes zero), and  $\alpha$  is a parameter which, for many smooth energy barriers, takes the value of 3/2 [26]. The energy barrier due to static random solutes, in the absence of any solute diffusion, can be derived from analytical considerations [27, 28]. Recent molecular dynamics and statics simulations for Al-Mg have reinforced these analytic models and provide some values for the parameters [26, 29]. The numerical simulations coupled with analytic studies performed for Al/5%-Mg alloys reveal approximate values for the non-dimensional parameter of  $\frac{\Delta E_0}{kT} \approx 71.4$  at room temperature,  $\tau_0 \approx 50 \text{ MPa}$ , and  $\alpha = 3/2$ .

When aging that acts to modify the energy barrier as a function of time, there are two models derivable from fundamental mechanisms under certain well-justified conditions. The first model prevails at low applied stresses when the spatial range of the diffusing solute cloud is smaller than the distance from the minimum to the maximum of the energy profile that exist before the aging commences and is given by

$$\Delta E(\tau, t) = \Delta E_0(\tau) + \Delta E_a(t) \quad (23)$$

where the second term is the additional energy barrier due to aging. The second model prevails at high stresses applied, when the spatial range of the solute cloud is greater than the distance between the minimum and maximum points of the energy profile, and is given by

$$\Delta E(\tau, t) = \Delta E_0(\tau - \Delta \tau_a(t)) \quad (24)$$

where  $\Delta \tau_a(t)$  is an effective time-dependent “back stress” opposing the dislocation motion due to solute diffusion. If the aging mechanism is dominated by the diffusion of the solute atoms towards the mobile dislocation cores when they are pinned at obstacles, then the energy barrier change can be represented by a form similar to Eq. 2 for the solute concentration as

$$\Delta E_a(t) = \Delta E_\infty \left( 1 - \exp \left( - \left( \frac{t}{t_d} \right)^n \right) \right) \quad (25)$$

where  $\Delta E_\infty$  is the saturation energy barrier change. A similar form can be derived for the aging-induced backstress, given by

$$\Delta \tau_a(t) = \Delta \tau_\infty \left( 1 - \exp \left( - \left( \frac{t}{t_d} \right)^n \right) \right) \quad (26)$$

where  $\Delta \tau_\infty$  is the saturation value of the strengthening due to the full formation of the solute cloud. A new model based on solute diffusion solely across the two planes on either side of the dislocation core, from tension to compression or vice-versa depending on the solute volume misfit, has been developed and justifies the forms of Eqs. 23-26 and provides explicit atomistically-derived formulas for all of the parameters [29]. Eqs. 23-26 are sufficiently general to represent other aging mechanisms and so our results here do not rely on the new model. Results for models using Eqs. 23 and 25 are remarkably similar to those obtained using Eqs. 24 and 26 and so we will confine our presentation of results to the case of Eqs. 24 and 26. For the cross-core diffusion mechanism described above [29], the saturation strengthening due to solute diffusion was estimated as  $\Delta \tau_\infty / \tau_0 \approx 0.1$  with  $n=1$ ,  $t_d \approx 6.3s$  at room temperature, and  $\Omega = 6.3 \cdot 10^{-4}$  [7, 21]. We use these values below for illustrative purposes, and describe the effects of a broader parameter study subsequently.

### 3.3 Steady-State Strain Rate Behavior

Predictions for the steady-state stress versus strain rate, via Eqs. 16-18, 24 and 26, are shown in Figure 1a for parameter values quoted in the previous section and for a selection of other values for some parameters. At high strain rates

$\dot{\epsilon} \gg \dot{\epsilon}_d = \Omega/t_d = 10^{-4} s^{-1}$ , the thermal escape occurs too quickly for the solute diffusion to occur and strengthen the system. The strain rate behavior is thus essentially that of a material with no aging effects, given by

$$\dot{\epsilon} = \nu_0 \Omega \exp\left(-\frac{\Delta E_0}{kT} \left(1 - \frac{\tau}{\tau_0}\right)^{3/2}\right), \quad (27)$$

as shown by the dotted line in Figure 1a. For slow strain rates  $\dot{\epsilon} \ll \dot{\epsilon}_d = \Omega/t_d = 10^{-4} s^{-1}$ , the thermal activation is so slow that the dislocations are fully aged prior to escape. The strain rate behavior is then that of a material with no aging effects, but shifted by the stress associated with the full aging, given by

$$\dot{\epsilon} = \nu_0 \Omega \exp\left(-\frac{\Delta E_0}{kT} \left(1 - \frac{\tau - \Delta\tau_\infty}{\tau_0}\right)^{3/2}\right) \quad (28)$$

as shown by the dash-dotted line in Figure 1a. The strain rate sensitivity in the regimes of high and low strain rates are

$$m = \frac{1}{\alpha} \frac{1}{\left(\frac{\Delta E}{kT}\right) - \left(\ln\left(\frac{\nu_0 \Omega}{\dot{\epsilon}}\right)\right)^{1/\alpha}} \left(\ln\left(\frac{\nu_0 \Omega}{\dot{\epsilon}}\right)\right)^{1/\alpha-1} \quad (29a)$$

and

$$m = \frac{1}{\alpha} \frac{1}{\left(1 + \frac{\Delta\tau_\infty}{\tau_0}\right) \left(\frac{\Delta E}{kT}\right) - \left(\ln\left(\frac{\nu_0 \Omega}{\dot{\epsilon}}\right)\right)^{1/\alpha}} \left(\ln\left(\frac{\nu_0 \Omega}{\dot{\epsilon}}\right)\right)^{1/\alpha-1} \quad (29b)$$

The variation of the strain rate sensitivity with the strain rate is shown in Figure 1b for each of the cases considered in Figure 1a.

At intermediate strain rates, there is a transition between the two limiting cases. The stress versus strain rate remains monotonically increasing, so that the strain rate sensitivity is always positive, as required by Eqs. 20 and 21. However, in this range of strain rates, the strain rate sensitivity is reduced substantially. For the parameters here, the strain rate sensitivity is reduced by up to a factor of 1/6 relative to the values at low strain rate. The aging thus does have a marked effect on the strain rate behavior of the material, increasing the strength with decreasing strain rate, but does not yield negative strain rate sensitivity. The reduction in strain rate sensitivity, however, can facilitate the onset of negative strain rate sensitivity if other mechanisms are included. The usual view of negative strain rate sensitivity is that the process with  $m < 0$  must overcome another process (the ‘‘normal’’ rate sensitivity) with  $m > 0$  to obtain a net parameter  $m < 0$ . The results here

show that the “normal” strain rate sensitivity itself is strongly reduced by the aging process, so that a weaker mechanism having  $m < 0$  can produce a net  $m < 0$ .

In spite of the complexity of the combination of Eqs.16-18 and 26, an accurate fully analytic expression for the strain-rate versus stress can be derived, as shown in Appendix 1. Thus, with some algebra only, any results for steady-state behavior as a function of any parameters in the model can be assessed quite rapidly.

Figures 1a,b also show the stress and strain rate sensitivity for a few combinations of material parameters. Parameter variations change the detailed results but not the general conclusions or the limiting cases. Increasing or decreasing the saturation aging stress, which can depend on the type and concentration of the mobile solute atom, increases or decreases the low-strain-rate stresses. Moreover, the value of the saturation aging stress determines the point at which the asymptotic low-strain-rate limit is achieved. In Figure 1a, we see that increasing  $\Delta\tau_\infty$  from  $0.1\tau_0$  to  $0.15\tau_0$  shifts the asymptotic limit from  $\dot{\epsilon}/\dot{\epsilon}_d \approx 10^{-3} s^{-1}$  to  $\dot{\epsilon}/\dot{\epsilon}_d \approx 10^{-5} s^{-1}$ , and flattens the stress response to generate a wider range of lower strain rate sensitivity (Figure 1b). Changing the parameter  $n$  from 1 to 1/3, a common range assumed in many models, broadens the transition range at higher stresses but with a corresponding increase in the strain-rate-sensitivity over the DSA range.

### 3.4 Non-steady State Response: Strain Rate Jump Tests

As noted earlier, obtaining the correct transient behavior during strain-rate jumps is essential for any proper numerical modeling of PLC-type instabilities. In addition, strain-rate jump tests are a common method for extracting steady-state strain rate sensitivity. Here we demonstrate that the model of Eqs.12 and 17 shows the expected physical behavior of an instantaneous positive strain rate sensitivity upon a jump in the strain rate followed by a relaxation to the steady-state stress at the new strain rate. Although there is no negative SRS, the transient behavior is important. In addition, strain-rate jump experiments aimed at understanding dynamic strain aging have been performed in the stable ( $m > 0$ ) low-strain-rate regime so that the entire deformation process is homogeneous and well-defined [6, 30]. These experiments still show transient behavior and aging effects, and it is necessary that these effects be captured properly in a model.

Imagine a system in steady state at constant strain rate  $\dot{\epsilon}_1$  for times  $t < 0$  that is then subjected to an instantaneous strain rate change to  $\dot{\epsilon}_2$  at  $t = 0$ . At much later times, the system should attain a new steady state at stress  $\tau(t) = \tau_2$  where  $\tau_2$  is the stress required to maintain the steady-state strain rate  $\dot{\epsilon}_2$ . We are interested in predicting the stress history  $\tau(t)$   $t \geq 0$ . For the specified strain jump, Eq. 12 requires the strain history to satisfy

$$\begin{aligned} \dot{\epsilon}_2 = & \int_{-\infty}^0 \dot{\epsilon}_1 \nu(\tau(t), t - t_p) \exp\left(-\int_{t_p}^t \nu(\tau(t'), t' - t_p) dt'\right) dt_p + \\ & + \int_0^t \dot{\epsilon}_2 \nu(\tau(t), t - t_p) \exp\left(-\int_{t_p}^t \nu(\tau(t'), t' - t_p) dt'\right) dt_p \end{aligned} \quad (30a)$$

For the same test, Eq. 17 predicts a stress history obeying

$$\Omega = \int_{-\infty}^0 \dot{\epsilon}_1 \exp\left(-\int_{t_p}^t \nu(\tau(t'), t'-t_p) dt'\right) dt_p + \int_0^t \dot{\epsilon}_2 \exp\left(-\int_{t_p}^t \nu(\tau(t'), t'-t_p) dt'\right) dt_p \quad (30b)$$

In the above equations, there are two classes of dislocations: those pinned before  $t = 0$  and those pinned after  $t=0$ . However, the time evolution of the energy barrier due to diffusion is independent of such a distinction. The solutes accumulate on a given dislocation starting at  $t_p$  and continuing until the dislocation escapes. During the pinning time, the strain rate and stress can be changing, but the dislocation energy barrier itself is only varying with the stress. The only exception to this would be if the change in applied stress changes the local dislocation position and thereby changes the solute cloud evolution by resetting the pinning time without having caused any appreciable strain increment; we neglect such a possibility, which has never yet been considered.

In the absence of aging, Eq. 30a predicts the expected result. The rate of escape is independent of the pinning time and so at time  $t = 0^+$ , Eq. 30a requires

$$\dot{\epsilon}_2 / \dot{\epsilon}_1 = \nu(\tau(0^+)) / \nu(\tau_1) \quad (31)$$

This requires further  $\tau(0^+) = \tau_2$  since  $\dot{\epsilon}_1 = \Omega \nu(\tau_1)$ . In other words, the stress immediately jumps to the value necessary to maintain the newly imposed rate  $\dot{\epsilon}_2$ . The stress then stays fixed at this value, with no transient behavior. This is the required and expected result because in the absence of aging the dislocations possess no memory of their residence at the pinned location. The dislocation escape is purely a stochastic phenomenon depending on the instantaneous applied stress. There is thus no transient behavior.

In the presence of aging, neither Eq. 30a nor Eq. 30b alone is suitable for obtaining numerically the entire stress history  $\tau(t)$  for  $t \geq 0$ . Immediately after the jump, the second term in Eq. 30b is negligible and provides no information about the instantaneous stress jump. Conversely, at long times the first term in Eq. 30a becomes negligible and Eq. 30a becomes an identity independent of the stress history. However Eqs. 30a, b enforced simultaneously for all times are able to capture the complete history. The numerical approach used here is described in Appendix 2.

The instantaneous jump in stress accompanying the jump in strain rate can be evaluated using Eq. 30a. Immediate after the jump, at  $t = 0^+$ , Eq. 30a requires the stress  $\tau(0^+)$  to satisfy

$$\dot{\epsilon}_2 / \dot{\epsilon}_1 = \nu(\tau(0^+), 0) / \nu(\tau_1, 0) + \int_0^\infty \frac{d}{dt} \left( \nu(\tau(0^+), t) / \nu(\tau_1, t) \right) \exp\left(-\int_0^t \nu(\tau_1, t') dt'\right) dt \quad (32)$$

The first term on the right hand side is similar to Eq. 31. The second term on the right hand side of Eq. 32 is negligible in comparison, being identically zero for  $\alpha = 1$  and 2-3 orders of magnitude smaller for  $\alpha = 3/2$ . Thus, to a very good approximation, the instantaneous stress satisfies

$$\dot{\epsilon}_2 / \dot{\epsilon}_1 \approx \nu(\tau(0^+), 0) / \nu(\tau_1, 0) \quad (33)$$

Using Eq. 6 for the rate of escape of a dislocation from the energy barrier given by Eq. 22 then yields

$$\ln\left(\frac{\dot{\epsilon}_2}{\dot{\epsilon}_1}\right) \approx -\frac{\Delta E_0}{kT} \left( \left(1 - \frac{\tau(0^+)}{\tau_0}\right)^\alpha - \left(1 - \frac{\tau_1}{\tau_0}\right)^\alpha \right) \quad (34)$$

The stress jump from  $\tau_1$  to  $\tau(0^+)$  is thus almost exactly the same as for the “no aging” case, because there is no time for solute diffusion to occur during the instantaneous jump. The starting value  $\tau_1$  is different, however, due to the aging mechanism.

After the jump in strain rate (and stress), the stress relaxes to the final steady state value. For jumps in the very low and very high strain rate regimes, the stress value jumps directly to the steady-state value and the transient is absent. For intermediate strain rates, the stress jumps to the value  $\tau(0^+)$  and evolves asymptotically to the steady state value. Figure 2a shows the stress jump and transient stress for a strain rate jump ratio of  $\dot{\epsilon}_2 / \dot{\epsilon}_1 = 10$  for a wide range of initial strain rates  $\dot{\epsilon}_1$ . Figure 2b shows the stress jump and transient stress for a strain rate jump downward of  $\dot{\epsilon}_2 / \dot{\epsilon}_1 = 1/10$ . The magnitude of the jump agrees well with Eq. 34 for both jumps up and jumps down in the strain rate. Although the transient behavior appears to be approximately exponential when viewed over the full time scale of the transient, in detail it is different. The rate of stress relaxation immediately after the jump is actually quite low. At slightly later times, the rate of relaxation increases very rapidly, appearing in Figure 2 as an abrupt change on the time scale shown. Eventually, the rate of relaxation transitions to something like an exponential decay. Thus, an exponential stress transient, as emerges in the standard model of Eqs. 2, 4, 5 is not entirely accurate. The predictions for the instantaneous material response immediately after the jump and its independence on the dynamic strain aging phenomena were also inferred in the by McCormick [2] and Hähner [1], but the latter solutions were based on the linear response of these Eqs. 12 and 17 leading to an asymptotic stress not equal to that corresponding to the steady state  $\dot{\epsilon}_2$  but instead depending on both  $\dot{\epsilon}_1$  and  $\dot{\epsilon}_2$ .

We estimate a transient time  $t^*$  by fitting  $\tau(t) - \tau_2$  for  $t \geq t_j$  to the form  $\bar{\tau} \left(1 - \exp\left(-\left(t/t^*\right)^p\right)\right)$ . The best-fit exponent  $p=2/3$  emerged in all cases. Figure 3 shows the value of  $t^*$ , normalized by  $t_d$ , as a function of the final strain rate  $\dot{\epsilon}_2$  normalized by  $\dot{\epsilon}_d$  for a wide range of strain rates and jumps up and down in rate by a factor of 10. In the model of McCormick [2], the transient time scales with the inverse of the final strain rate  $\dot{\epsilon}_2$  and so decreases continuously with increasing strain rate. In contrast, we find that the transient time is non-monotonic, with the transient time *increasing* up to a critical normalized strain rate between  $10^1 \dot{\epsilon}_d$  and  $10^2 \dot{\epsilon}_d \text{ s}^{-1}$ , followed by a fast decrease. Qualitatively similar non-monotonic results were found by Hähner [1] for jumps up in strain rate, but with quantitative differences. Figure 3 shows that the transient time is smaller for a jump down in the strain rates (from  $10\dot{\epsilon}_2$  to  $\dot{\epsilon}_2$ ) than for a jump up (from  $\dot{\epsilon}_2/10$  to  $\dot{\epsilon}_2$ ). This is expected because for a jump down, the waiting time is relatively smaller than for a jump up, so that the aging history is forgotten more quickly.

### 3.5 Non-steady State Response: Continuous Strain Rate History

Finally, we investigate the response of the material to a time-varying strain rate history. This exercise reveals that there are aging effects for non-steady-state and non-jump conditions that arise from the competition between the rate that solutes can diffuse to the dislocations and the time-varying rate of dislocation escape required to maintain the imposed strain history. We choose a simple periodic strain rate history, as might occur under cyclic fatigue conditions or under conditions of instability that could arise if other aging effects give negative SRS. Specifically, we impose a constant strain rate history up to time  $t = 0$  followed by a periodic variation in strain rate given by:

$$\dot{\epsilon}(t) = \begin{cases} \dot{\epsilon}_0 & t \leq 0 \\ \dot{\epsilon}_0 + \Delta\dot{\epsilon} \sin^2(\omega t) & t \geq 0 \end{cases} \quad (35)$$

Figure 4 shows three examples of stabilized stress-strain rate cycles for (i)  $\dot{\epsilon}_0 = 10^{-4} s^{-1}$ ,  $\Delta\dot{\epsilon} = 9 \cdot 10^{-4} s^{-1}$ ; (ii)  $\dot{\epsilon}_0 = 10^{-3} s$ ,  $\Delta\dot{\epsilon} = 9 \cdot 10^{-3} s$  and (iii)  $\dot{\epsilon}_0 = 10^{-2} s^{-1}$ ,  $\Delta\dot{\epsilon} = 9 \cdot 10^{-2} s^{-1}$ , all of them with a frequency of  $\pi/\omega = 100s$ . Numerically, the stress evolution was obtained using Eq. 12, which is accurate since the imposed strain rate is a continuous function. For each time increment, it was verified that Eq. 17 was also satisfied to within 2%. From Figure 4, we see that the value of the stress field at the end of the first cycle is lower than the initial steady state value although the strain rate is the same. This difference is indicated in Figure 4, with  $\delta_1 = 0.004$  for (i),  $\delta_2 = 0.006$  for (ii) and  $\delta_3 = 0.002$  for (iii). This behavior is due to the aging, and is not surprising if we consider the influence of the stress history. First, at the beginning and end of the cycle the strain rate is the same and so the instantaneous effects cancel during the history. When the interaction between the solutes and dislocations is included, the higher strain rate during cycling causes a lower average aging time, lower diffusion of the solutes across the dislocation core, and thus a lower value for the stress as compared to the initial steady-state. A similar experiment with the steady-state strain rate prior to the cycle higher than any of the strain rates during the cycling, a higher value peak stress (hardening) would arise. The same behavior can be also inferred qualitatively from the McCormick [2] model. With further cycling, the constant strain-rate prior to  $t=0$  is forgotten after some period that depends the details (initial strain rate, amplitude, and frequency) and the cyclic stress response stabilizes.

## 4. Conclusions

We have presented a kinetic model for a dynamic strain aging mechanism in solid solutions based on thermally activated release of the dislocations from their local pinning points, leading to constitutive equations for the stress versus strain rate in these materials. Most importantly, our analysis shows that the consideration of a single rate-dependent strengthening mechanism (e.g. mobile dislocations, temporary pinned and aged at various obstacles) can not lead to negative strain rate sensitivity. The aging mechanism does significantly lower the strain rate sensitivity in the DSA range of strain rates where the solute diffusion is an active process. This opens the possibility of negative strain rate sensitivity in the presence of other types of defects interactions (e.g. interactions between

dislocations junctions and solute atoms), which can be easily incorporated in our model through appropriate changes in the energetic barriers that must be overcome by thermal activation. The current model does predict the observed memory effects. For strain-rate jump tests within the DSA range, the material stress response shows an instantaneous response independent of any aging mechanisms followed by a transient regime, with convergence to the post-jump steady-state solution. The material memory within the DSA range is also shown for a cyclic strain-rate history, leading to apparent softening effects. With the ability to recover the classical kinetic theories in the absence of aging effects but also able to incorporate various dislocation/solute interactions mechanisms, the current model provides a robust rate-dependent constitutive equation for the solute strengthening and aging effects in metal alloys. In a companion paper, we consider the influence of forest strengthening, and forest aging, within the same fundamental framework, and show the emergence of negative strain rate sensitivity and a host of other phenomena typically observed in alloys exhibiting dynamic aging due to solute effects.

### Appendix 1.

Here, we derive an accurate analytic form for the steady-state average waiting time in Eq. 16, which then directly determines the steady-state strain rate versus stress via Eq. 18, when the time-dependent energy barrier is given by Eqs.24, 26. Similar results can be obtained using Eqs.23, 25. We divide the integration domains in Eq. 16 into three regions ( $[0, (1-k)t_d]$ ,  $[(1-k)t_d, (1+k)t_d]$ ,  $[(1+k)t_d, \infty]$ ), where  $k$  is a parameter, and approximate each of the integrals in the selected interval. The division into three regions leads to the exact result

$$\begin{aligned} \bar{t}_w = \int_0^{\infty} \exp\left(-\int_0^t v(\tau, t') dt'\right) dt &= \int_0^{(1-k)t_d} \exp\left(-\int_0^t v(\tau, t') dt'\right) dt + \\ &+ \int_{(1-k)t_d}^{(1+k)t_d} \exp\left(-\int_0^{(1-k)t_d} v(\tau, t') dt' - \int_{(1-k)t_d}^t v(\tau, t') dt'\right) dt + \\ &+ \int_{(1+k)t_d}^{\infty} \exp\left(-\int_0^{(1-k)t_d} v(\tau, t') dt' - \int_{(1-k)t_d}^{(1+k)t_d} v(\tau, t') dt' - \int_{(1+k)t_d}^t v(\tau, t') dt'\right) dt \end{aligned} \quad (\text{A1.1})$$

We then make the following approximations:

- (i) On the interval  $[0, (1-k)t_d]$ , assume  $t^m \ll t_d^n$ , so that the rate of escape at the time  $t'$  is estimated as

$$v(\tau, t') \cong v_0 \left( 1 - \alpha \left( 1 - \frac{\tau}{\tau_0} \right)^{\alpha-1} \frac{\Delta\tau_{\infty}}{\tau_0} \frac{\Delta E_0}{kT} \left( \frac{t'}{t_d} \right)^n \right) \exp\left( -\frac{\Delta E_0}{kT} \left( 1 - \frac{\tau}{\tau_0} \right)^{\alpha} \right) \quad (\text{A1.2})$$

- (ii) On the interval  $[(1-k)t_d, (1+k)t_d]$ , assume  $t^m \cong t_d^n$  and approximate the rate of escape as

$$v(\tau, t') \cong v_0 \left( 1 + \theta \left( 1 - \left( \frac{t'}{t_d} \right)^n \right) \right) \exp \left( - \frac{\Delta E_0}{kT} \left( 1 - \frac{\tau}{\tau_0} + \left( 1 - \frac{1}{e} \right) \frac{\Delta \tau_\infty}{\tau_0} \right)^\alpha \right) \quad (\text{A1.3})$$

where  $\theta = \frac{1}{e} \alpha \left( 1 - \frac{\tau}{\tau_0} + \left( 1 - \frac{1}{e} \right) \frac{\Delta \tau_\infty}{\tau_0} \right)^{\alpha-1} \frac{\Delta \tau_\infty}{\tau_0} \frac{\Delta E_0}{kT}$  and  $e = \exp(1)$ .

- (iii) On the interval  $[(1+k)t_d, \infty]$ , assume  $t^m \gg t_d^n$  and thus approximate the rate of escape as

$$v(\tau, t') \cong v_0 \exp \left( - \frac{\Delta E_0}{kT} \left( 1 - \frac{\tau}{\tau_0} + \frac{\Delta \tau_\infty}{\tau_0} \right)^\alpha \right) \quad (\text{A1.4})$$

Substituting the approximations of (A1.2-4) into each of the integrals in (A1.1) leads to a waiting time that can be written in the form

$$\bar{t}_w = t_0 D_0 + t_1 D_1 + t_\infty D_\infty \quad (\text{A1.5})$$

where

$$t_0 = \left( v_0 \exp \left( - \frac{\Delta E_0}{kT} \left( 1 - \frac{\tau}{\tau_0} \right)^\alpha \right) \right)^{-1}$$

$$t_1 = \left( v_0 \left( 1 + \frac{n}{n+1} 0.36 \alpha \left( 1 - \frac{\tau}{\tau_0} + 0.63 \frac{\Delta \tau_\infty}{\tau_0} \right)^{\alpha-1} \frac{\Delta \tau_\infty}{\tau_0} \frac{\Delta E_0}{kT} \right) \exp \left( - \frac{\Delta E_0}{kT} \left( 1 - \frac{\tau}{\tau_0} + 0.63 \frac{\Delta \tau_\infty}{\tau_0} \right)^\alpha \right) \right)^{-1}$$

$$t_\infty = \left( v_0 \exp \left( - \frac{\Delta E_0}{kT} \left( 1 - \frac{\tau}{\tau_0} + \frac{\Delta \tau_\infty}{\tau_0} \right)^\alpha \right) \right)^{-1}$$

$$D_0 = 1 - \exp \left( - (1-k) \frac{t_d}{t_0} \right),$$

$$D_\infty = \exp \left( - (1-k) \frac{t_d}{t_0} - 2k \frac{t_d}{t_1} \right)$$

$$D_1 = 1 - D_0 - D_\infty.$$

Figure A1 shows the relative error  $|\tau - \tau^{approx}| / \tau$  versus normalized strain rate for this approximation, where  $\tau$  is the steady-state stress computed numerically via Eq.16 and

$\tau^{approx}$  is computed using Eq.A1.5 with  $k=0.95$ . The error is less than 3.5% for  $n=1/3$  and less than 1.5% for  $n=1$ . The approximation can be further improved by optimizing  $k$  for each  $n$ .

## Appendix 2.

Here we provide additional details about the numerical procedures used in the determination of the material response to an imposed instantaneous jump in the strain rate. As mentioned in Section 3.3, neither Eq. 30a nor Eq. 30b can be used alone for accurate predictions of the stress response for the entire history of deformation. Nevertheless, both Eqs.30a, b must be simultaneously satisfied. It can be easily observed that the Eq.30a can be replaced by:

$$\begin{aligned} \dot{\epsilon}_2 = h \left[ \int_{-\infty}^0 \dot{\epsilon}_1 v(\tau(t), t - t_p) \exp\left(-\int_{t_p}^t v(\tau(t'), t' - t_p) dt'\right) dt_p + \right. \\ \left. + \int_0^t \dot{\epsilon}_2 v(\tau(t), t - t_p) \exp\left(-\int_{t_p}^t v(\tau(t'), t' - t_p) dt'\right) dt_p \right] \end{aligned} \quad (A2.1)$$

where

$$h = \Omega / \left[ \int_{-\infty}^0 \dot{\epsilon}_1 \exp\left(-\int_{t_p}^t v(\tau(t'), t' - t_p) dt'\right) dt_p + \int_0^t \dot{\epsilon}_2 \exp\left(-\int_{t_p}^t v(\tau(t'), t' - t_p) dt'\right) dt_p \right] \quad (A2.2)$$

which does not reduce to an identity in the steady-state regime. Prior to the jump time Eqs.A2.1, 2.2 reduce to Eq. 17, which can be easily solved. Then, starting from the jump time, the time interval is discretized into small increments  $[t_0, t_1, \dots, t_k, \dots]$ . Eq. A2.1 is then solved consecutively for each discretized value. Given the stress computed at times  $[t_0, t_1, \dots, t_{k-1}]$  and making linear interpolations between these increments, we predict the stress at  $t=t_k$  by solving a nonlinear equation for the unknown  $\tau_k = \tau(t_k)$  using linear extrapolation in the interval  $[t_{k-1}, t_k]$  as  $\tau(t') = \tau_{k-1} + (\tau_k - \tau_{k-1})(t_{k-1} - t') / (t_k - t_{k-1})$ . The convergence of the solution for each time  $t_k$  depends on the increment  $t_k - t_{k-1}$ . Eq. A2.1 allows moderate time increments, about 1/100 of the transient time, to be used. After solving Eq. A2.1, Eq. 30a and 30b are then numerically verified at each time increment. We note that the solution depends on the lower limit in Eq. A2.1, which theoretically is  $-\infty$  but can be set to  $-1/\dot{\epsilon}_1$  while maintaining accurate solutions.

## Acknowledgements

The authors acknowledge support of this work through the General Motors/Brown Collaborative Research Laboratory on Computational Materials Science and the NSF Materials Science Research and Engineering Center on ‘‘Nano and Micromechanics of Materials’’ at Brown University, grant # DMR-0520651. The authors thank Prof. C. Picu for useful discussions. WAC thanks Prof. A. Benallal for conversations that led to the initiation of this work, performed while WAC was a Visiting Professor at LMT, Ecole Normale Supérieure de Cachan.

## References

- [1] Hähner P, *Mat. Sci. Eng. A* 1996, 207: 208.
- [2] McCormick PG, *Acta Metall.* 1988, 36: 3061-3067.
- [3] Estrin Y, McCormick PG, *Acta Metall. Mater.* 1991, 39(12):2977.
- [4] Kocks UF, Argon AS, Ashby MF, *Prog. Mat. Sci.* 1975, 19:1.
- [5] Hanson K, Morris JW, *J. Appl. Phys.* 1975, 46:2378.
- [6] Springer F, Nortmann A, Schwink Ch, *Phys. Stat. Sol. (a)*, 1998, 170:63.
- [7] Kubin LP, Estrin Y, *Acta Metall. Mater.* 1990, 38(5): 697.
- [8] Balík J, Lukáč P, *Acta Metall. Mater.* 1993, 41:1447.
- [9] Friedel, J. 1964. *Dislocations*. Pergamon Press. Oxford.
- [10]Caillard D, Martin JL, *Thermally Activated Mechanisms in Crystal Plasticity*. Elsevier, 2003.
- [11]Cottrell AH, Stokes RJ. *Proc. Royal Soc. London. Series A, Math. and Phys. Sci.* 1955; 233: 17.
- [12] Zhu T, Li J, Samantha A, Kim HG, Suresh S, *PNAS*, 2006, 104(9):3031.
- [13] Swygenhoven Van H, Caro A, *Phys. Rev.B*, 1998, 58(17): 11246.
- [14] Van den Beukel A, *Phys. Stat. Sol. A* 1975, 30:197.
- [15] Mulford A, Kocks UF, *Acta Metall.* 1979, 27:1125.
- [16] Neuhauser H, Schwink C, *Solid Solution Strengthening*, In Cahn RW, Haasen P, Kramer EJ editors. *Mat. Sci. Tech. A Comprehensive Treatment, Plastic Deformation and Fracture of Materials*, VCH, Weinheim, Germany, 1993, 6:191.
- [17] Kubin LP, Chihab K, Estrin Y., 1987. Nonuniform plastic deformation and the Portevin-Le Châtelier effect. In *Patterns, Defects and Microstructures in Nonequilibrium Systems*; Austin, Texas; USA; 24-28 Mar. 1986, 220.
- [18] Rizzi E, Hahner P, *Int. J. Plasticity* 2004; 20:121.
- [19] Hähner P, *Acta Mater.* 1997, 45(9):3695.
- [20] Hähner P, Ziegenbein A, Rizzi E, Neuhäuser H, *Phys. Rev.B* 2002, 65:134109-1-20.
- [21] Kubin LP, Estrin Y, Perrier C, *Acta Metall. Mater.* 1992, 40(5):1037.
- [22] Ling CP, McCormick PG, *Acta Metall. Mater.* 1990, 38:2631.
- [23] Ling CP, McCormick PG, *Acta Metall. Mater.* 1993, 41(11):3127.
- [24] Scher H, Shlesinger MF, Bender JT, *Physics Today* 1991, 44(1):26.
- [25] Zaiser M, Hahner P, *Mat. Sci. Eng.* 1997, A238:399.
- [26] Olmsted DL, Hector LG, Curtin WA, *J. Mech. Phys. Sol.* 2006, 54: 1763.
- [27] Labush R, *Phys. Status Solidi*, 1970, 41(2): 659.
- [28] Zaiser M, *Phil. Mag. A* 2002, 82(15):2869.
- [29] Curtin AW, Olmsted DL, Hector LG, *Nature Materials* 2006, 5: 875.
- [30] Schwink Ch, Nortmann A, In *Plasticity of Metals*. Eds. Elmar Steck, Reinhold Ritter, Udo Peil, Alf Ziegenbein, Wiley-VCH Verlag GmbH, 2001, 5:90.

## Figure Captions

Figure 1. a) Non-dimensional stress versus normalized strain rate, as predicted by Eqs.16, 18, 27, and 28, for various sets of material parameters. The normalizing constant for the strain rate is  $\dot{\epsilon}_d = \Omega/t_d = 10^{-4} / s$ . b) Strain rate sensitivity  $m = \log(\tau)/\log(\dot{\epsilon})$  versus normalized strain rate as predicted for various material parameters corresponding to those in a).

Figure 2. Non-dimensional stress versus time, as predicted for strain-rate jump tests with  $\dot{\epsilon}_2 / \dot{\epsilon}_1 = 10$  at time  $t_j$  and within the DSA range of strain rates. The jump time  $t_j$  is selected to have different values for different initial strain rates for a better visualization. Each curve shows the steady-state value corresponding to  $\dot{\epsilon}_1$  prior to  $t_j$ , an instantaneous jump at  $t_j$ , and a transient decrease toward the steady state stress for  $\dot{\epsilon}_2$ .

Figure 3. Estimated transient time  $t^*$  (normalized by  $t_d$ ) after a strain rate jump versus normalized strain rate, for strain rate jump ratios of  $\dot{\epsilon}_2 / \dot{\epsilon}_1 = 10$  and  $\dot{\epsilon}_2 / \dot{\epsilon}_1 = 1/10$ .

Figure 4. Non-dimensional stress versus strain rate versus strain rate history for  $t > 0$ , for several sets of histories described by Eq. 35 with parameters ( $\dot{\epsilon}_0 = 10^{-4} s^{-1}$ ,  $\Delta\dot{\epsilon}_0 = 9 \cdot 10^{-4} s^{-1}$ ), ( $\dot{\epsilon}_0 = 10^{-3} s^{-1}$ ,  $\Delta\dot{\epsilon}_0 = 9 \cdot 10^{-3} s^{-1}$ ), and ( $\dot{\epsilon}_0 = 10^{-2} s^{-1}$ ,  $\Delta\dot{\epsilon}_0 = 9 \cdot 10^{-2} s^{-1}$ ), and  $\omega = \pi/100 s^{-1}$  for all cases.

Figure A1. Variation of the relative error in the stress,  $|\tau - \tau^{approx}| / \tau$ , versus normalized strain rate, where  $\tau$  is the steady-state stress computed using Eq.16 and  $\tau^{approx}$  is computed using Eq.A1.5 with  $k=0.95$ .

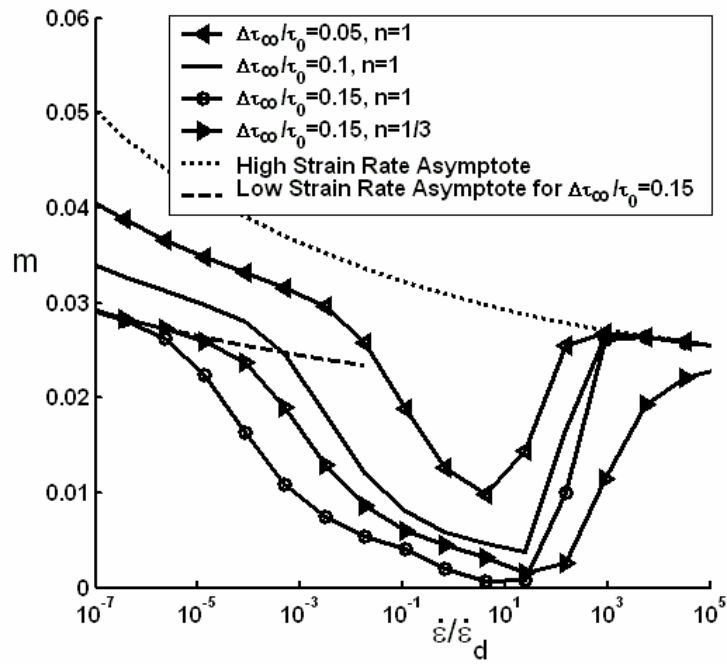
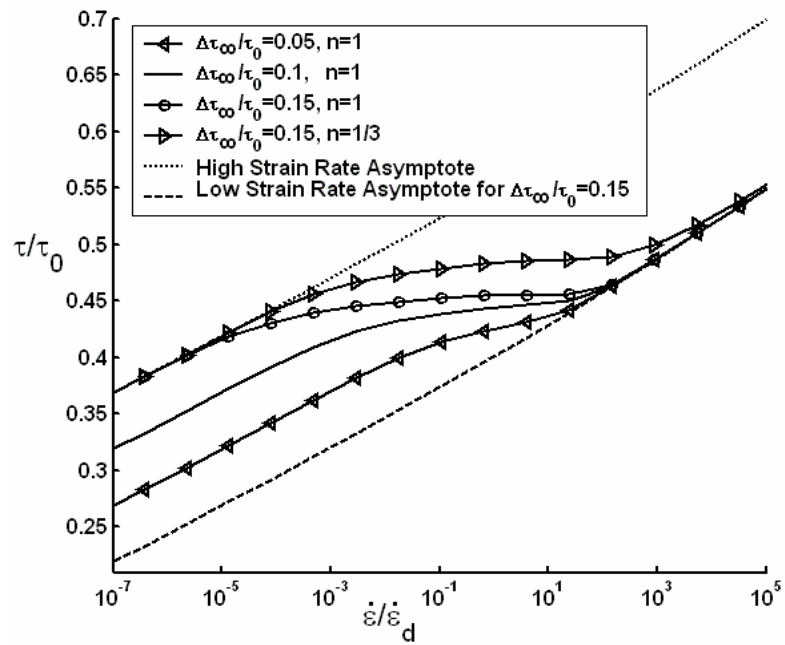


Figure 1 a), b)

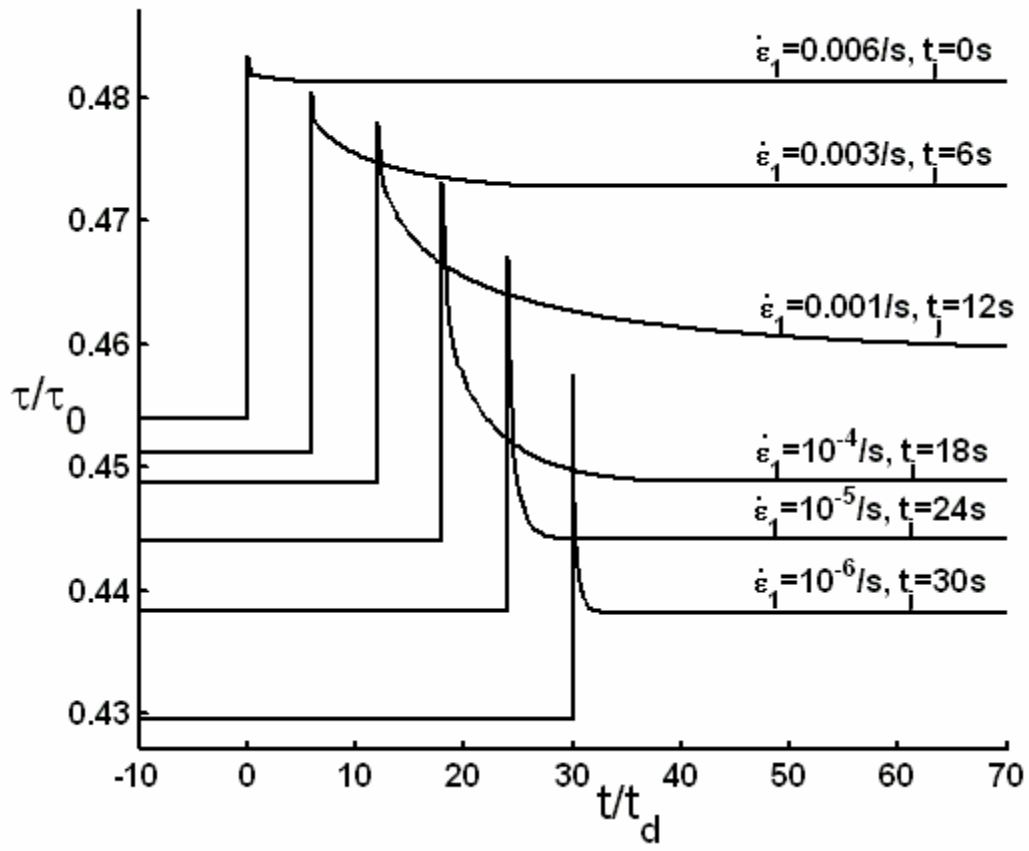


Figure 2

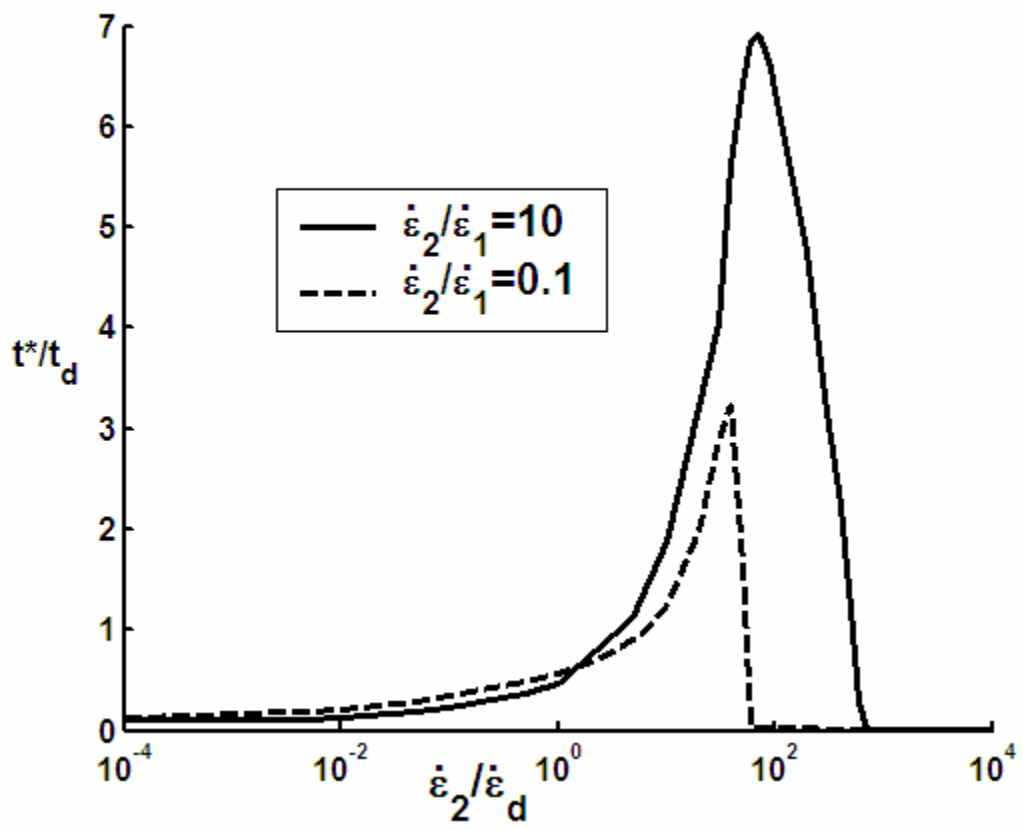


Figure 3

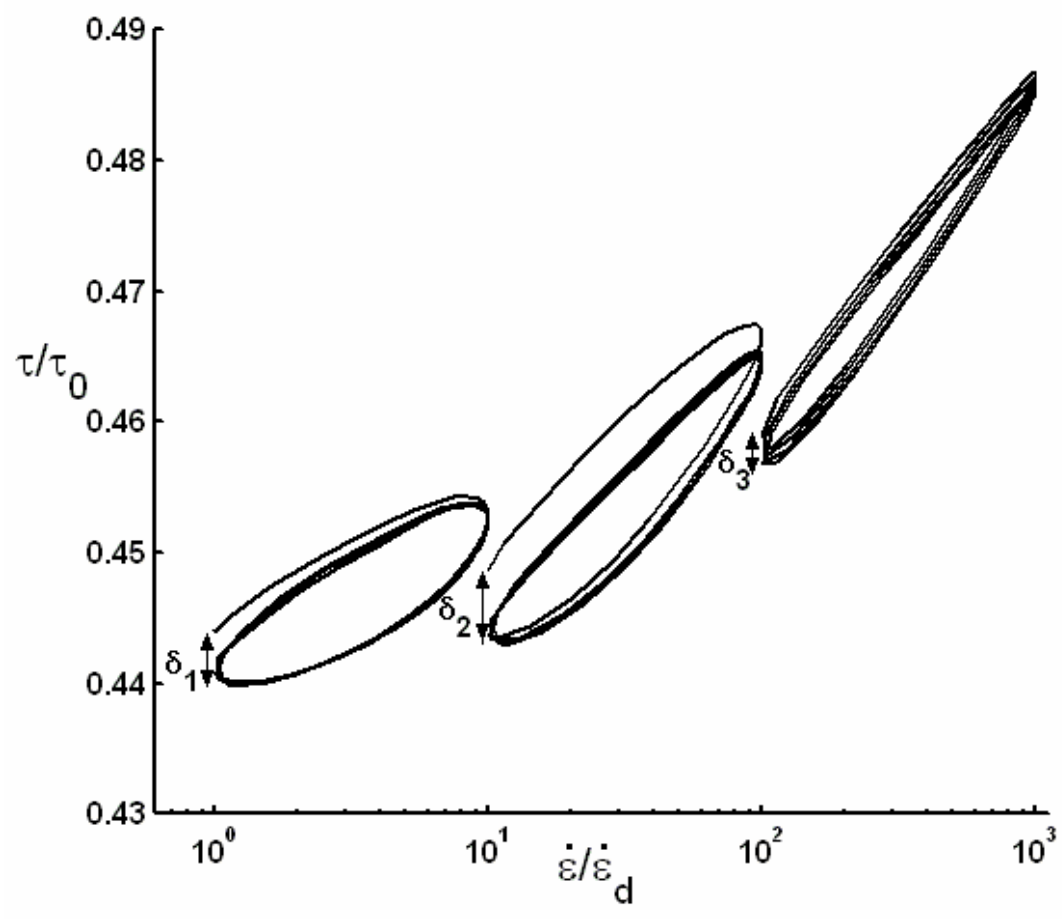


Figure 4

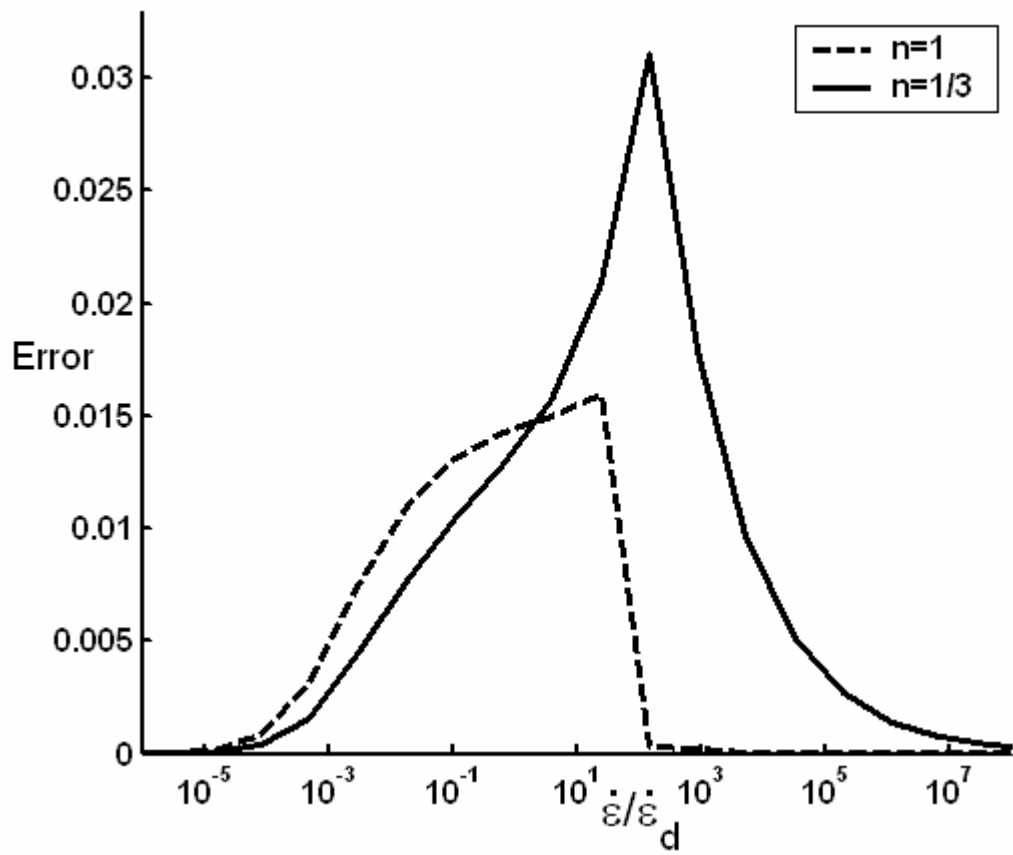


Figure A1